Phase difference between normal and shear forces during tactile exploration represents textural features

Hikaru Hasegawa, Shogo Okamoto, and Yoji Yamada

***Abstract*—Contact forces and skin deformation induced during tactile exploration have been investigated in the frequency domain to understand finger–material interaction. Their power spectra are one of the representative feature quantities that have been associated with the surface properties of materials. However, thus far, the phase information of these quantities has not been studied. Furthermore, most previous studies focused on uni-dimensional signals such as forces in either the normal or tangential directions. We investigated the phase differences between normal and shear forces induced during tactile exploration. The results showed that the phase differences between these two axial forces differ among materials and that they exhibit features different from their power spectra. These results indicate that the phase difference between two axial forces should be taken into account to understand the finger–material interactions during tactile exploration.**

***Index Terms*—Phase difference, Normal and shear forces, Power spectrum, Tactile exploration.**

I. Introduction

HUMANS perceive textures by sliding their fingers on the material's surface, and this process relies on finger–material mechanical interaction. Different materials yield different interactions. Most previous studies analyzed the forces (e.g., [1], [2], [3], [4], [5], [6]) and skin deformation (e.g., [7], [8]) or vibration (e.g., [9], [10], [11], [12]) induced during tactile exploration, and found that they depended on the surface properties of the respective materials. Furthermore, the relationships between the forces or skin deformation and the subjective evaluation of materials have been investigated [13], [14], [15]. Thus, as indicated above, many studies have analyzed the mechanical phenomena associated with tactile exploration.

Mechanical signals such as contact forces or skin deformation caused by tactile exploration have been investigated in the frequency domain by many researchers. In particular, their power spectra are the representative feature quantities associated with the surface properties of the materials. For instance, it has been reported that 55 types of materials have been classified by the power spectra of skin vibrations [11]. The differences in these spectra correspond to the perceptual differences among the materials [9], [14], [15], [16]. Moreover, the materials could be classified by the power spectra of vibrations when they were scanned with a probe [17], [18], [19] or tactile sensors (e.g., [20], [21], [22], [23]). The differences in the surface properties of materials can be represented by the power spectra of mechanical signals observed when sliding the finger, probe or, tactile sensor on them.

Not only the power spectrum but also the phase spectrum can be computed by frequency analysis. However, the latter aspect has not been investigated thoroughly. The phases of mechanical signals induced during tactile exploration have never been investigated whereas some related studies focused on discriminating phases of vibrotactile components [24], [25], [26], [27]. It should be noted that the phases defined in these studies are the shifts between two sinusoidal waves with different frequencies that compose the stimuli. Some of these studies reported that the phases of high-frequency vibrotactile stimuli are difficult for humans to discriminate, and therefore, the phases of forces applied to the skin may not influence the perception of fine textures [24], [25]. The peak vibratory acceleration that is determined by the phases may influence the discrimination of high-frequency vibrotactile stimuli including several frequency components rather than their amplitudes or frequencies [26]. Also, the phases of low-frequency vibrotactile stimuli can be discriminated [24], [27]. Therefore, the effects of phases on texture perception may not be ignored. Nonetheless, little knowledge exists about phase spectra involving many frequency components; to date, no study has investigated the phases of forces or skin deformation induced during tactile exploration.

Uni-dimensional signals were the analysis target in the studies mentioned above. Although the forces or skin deformation are multi-dimensional or multidirectional, the relationships between them have not been studied. Thus far, the power spectra of skin vibrations and forces in a single direction or the coefficient of friction (defined as the ratio between the normal and shear forces) have been discussed. Our previous study [28] showed that the stochastic relationships between two axial forces differ among materials. This result suggests that the surface properties of materials may influence the relationships between the mechanical signals in multidirections. However, again, these relationships have not been investigated thoroughly. Consequently, the phase difference between multidirectional signals is a new perspective in this area.

To fill these gaps in the literature, we measured the normal and shear forces during tactile exploration in this study, and investigated whether their phase differences differ among materials. Then, we compared the material classification performance using phase differences between two axial forces and the power spectra of the forces in a single direction (shear force was selected in this study). We discussed the results from the viewpoint of phase differences, which represent causal relationships in physics between two axial forces, and expanded on their statistical properties [28]. As stated previously, despite its importance, phase difference, as an index, has not received much academic attention; thus, this is the first study to investigate the relationships between the phase difference between two axial forces and materials.

II. Experiment

We measured the normal and shear forces as well as finger positions during tactile exploration using one sample of each material. The total number of samples amounted to 19. The apparatus and materials used in the measurements were the same as those in [28]. However, in this study, the measurements were conducted with a larger number of participants.

A. Measurement setup

The device shown in Fig. 1 was used for measuring the two axial forces. Similar devices were used in previous studies [29], [30]. Two load cells (9313AA2, Kistler, Switzerland) were located on the bottom of the device for measuring the normal force. The shear

All authors are with the Department of Mechanical Systems Engineering, Nagoya University, Furo-cho, Chikusa-ku, Japan.

This work was partly supported by MEXT KAKENHI (17H04697 and 15H05923).

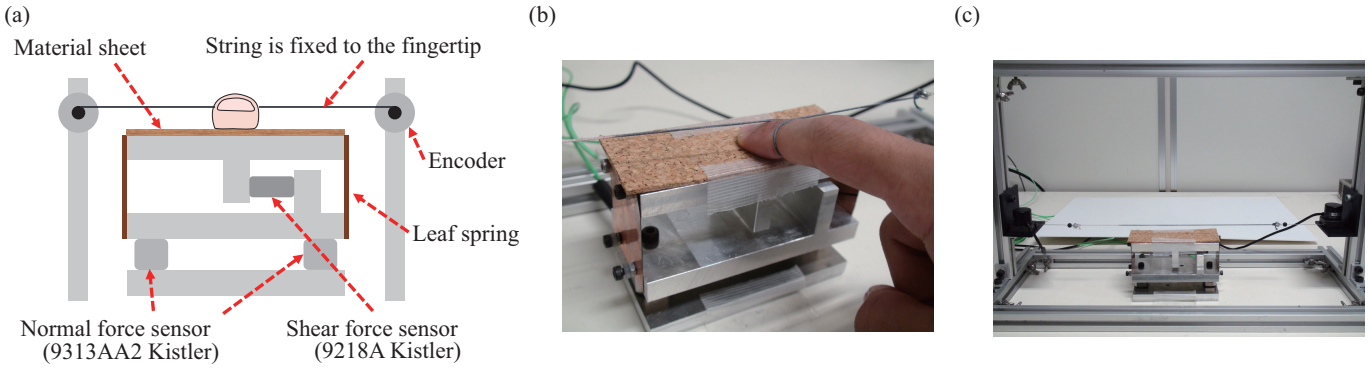

Fig. 1. (a) Schematic view, and (b) and (c) photographs of the force measurement setup.

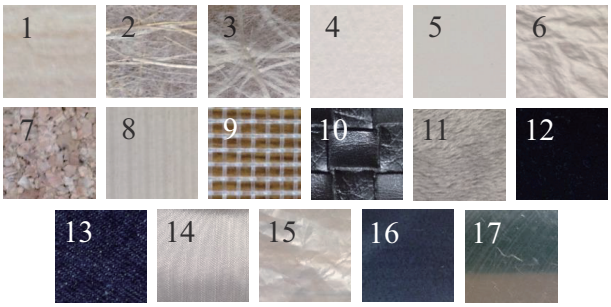

Fig. 2. Photographs of materials. The numbers correspond to those in Table I.

TABLE I
MATERIALS USED IN THE EXPERIMENT.

1. Wood	11. Fur
2. Coarse Japanese paper	12. Felt
3. Fine Japanese paper	13. Denim
4. Drawing paper	14. Polyester cloth
5. Coated paper	15. Polyethylene sheet
6. Crumpled paper	16. Rubber
7. Cork	17. Aluminum
8. Corrugated paper	18. Cork with talc
9. Woven resin wire mesh	19. Coarse Japanese paper with talc
10. Fake leather	

force was measured by a high-precision load cell (9217A, Kistler, Switzerland). The leaf spring fixed to the side of the device decoupled the two axial forces. The outputs of the normal and shear force sensors were amplified by two charge amplifiers (5073A and 5015, respectively; Kistler, Switzerland), and transferred to the computer at the sampling frequency as 2 kHz. The material sheets were fixed on the top surface of the device.

The finger position was measured by two-wire encoders (MTL-12, MTL Co., Japan). The wires were fixed on the fingertip, and thus, the encoders rotated along with the finger movements. The total tension applied to the fingertip by the two wires was canceled because they pulled in a crosswise direction.

B. Nineteen materials

We measured the forces using the materials that can be touched in our daily lives to investigate the aspects associated with natural tactile exploration. Fig. 2 shows the materials used in the experiment. Among them, cork and coarse Japanese paper induced strong friction. Thus, we prepared another pair of the same materials by lubricating their surfaces with talc. The 19 materials that were used in this study are shown in Table I.

C. Tasks

Participants actively slid their dominant index fingers over the materials fixed on the top surface of the device, as shown in Fig. 1 (b). They were instructed to stroke the surface in one direction for 20 s for each material. They wiped their fingers before each trial to eliminate surplus moisture. They could see the materials during trials, and the scanning speed and strength could be adjusted independently so as to perceive the quality of each material's surface and allow natural tactile exploration. However, we only used data corresponding to finger speeds ranging from 30–90 mm/s in the analysis that followed. In this speed range, a satisfactory amount of force data were available for computing the Fourier transforms for all participants.

D. Participants

Fourteen students (12 males and 2 females in their twenties) who were unaware of the objective of the study participated voluntarily in this experiment.

III. DATA ANALYSIS

We computed the phase differences between the normal and shear forces. We also computed the power spectra of the shear forces because they could be measured more precisely than those of the normal forces. The data when the finger speed ranged from 30–90 mm/s were analyzed. Frequency components higher than 300 Hz were excluded from the analysis because of the problems resulting from the signal-to-noise ratio.

A. Computation of phase difference between normal and shear forces

Let $F_n(t)$ and $F_s(t)$ be the time series data of the normal and shear forces, respectively. Then, their phase difference ϕ can be computed using

$$\phi(f) = \angle\left(\frac{\mathscr{F}\{F_s(t)\}}{\mathscr{F}\{F_n(t)\}}\right), \tag{1}$$

where f and $\mathscr{F}$ denote the frequency and Fourier transform, respectively. The phase difference ϕ is defined as the phase shift of the shear force against the normal force, and its value varies in the range of $(-\pi, \pi)$. When $\phi > 0$, the phase of the shear force leads that of the normal force. The sample numbers of $F_n(t)$ and $F_s(t)$ in each trial were larger than 2000 points, and they were thus downsampled so that the frequency resolutions of their spectra became 1 Hz ($\Delta f = 1$ Hz). To minimize the effect of noise, a moving average filter was applied to the computed phase differences (filter size: 10). Fig. 3 (a) shows an example of the phase difference between the two axial forces, induced by stroking corrugated paper.

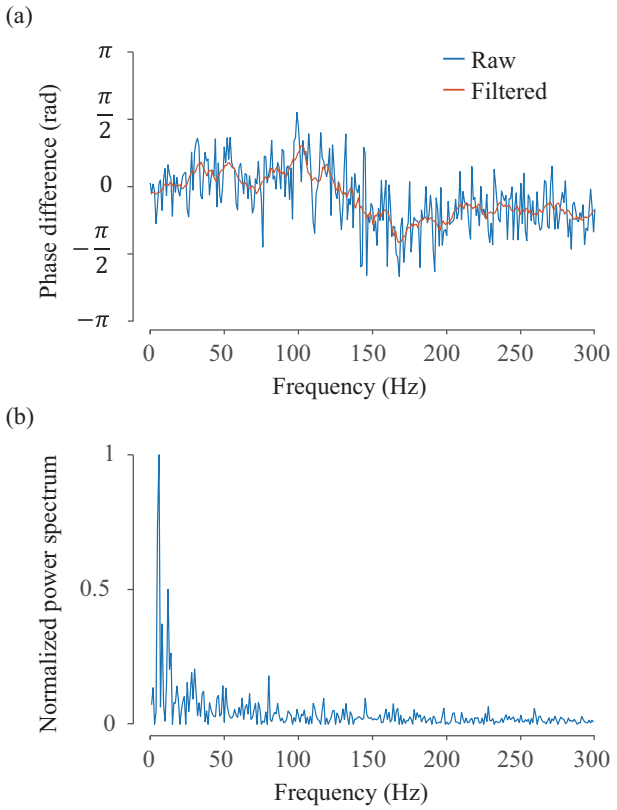

Fig. 3. Examples of the phase and power spectra of forces induced during tactile exploration. (a) Phase difference between two axial forces induced by stroking corrugated paper. The blue line denotes the raw spectrum. The orange line refers to the spectrum after applying a tenth-order moving average filter. (b) Normalized power spectrum of shear force induced by stroking cork.

B. Computation of power spectrum of shear force

We computed the power spectrum of shear force $P(f)$ with $\Delta f =$ 1 Hz and the data in the range of 1–300 Hz. In order to compare the profiles of the power spectra, $P(f)$ was normalized by the maximum value in each trial. Fig. 3 (b) shows an example of a power spectrum of the shear force, which was induced by stroking cork.

C. Feature vector extraction from spectra

We regarded the phase differences and power spectra as multivariate data, and applied a combination of principal component analysis (PCA) and linear discriminant analysis (LDA) [31] (*eig* function of Matlab 2019a, Mathworks Inc., MA) to compute the feature vectors that classify the materials. The PCA functions as a filter by removing the noise from each sample, and the LDA classifies them.

In LDA, the feature vectors that classify groups of samples are computed from two criteria measures. The first measure concerns the within-material scatter matrix $\boldsymbol{S}_w$. $\boldsymbol{S}_w$ of a sample set composed of m dimensional vectors that store the spectra can be defined as

$$\boldsymbol{S}_w = \sum_{j=1}^{c}\sum_{i=1}^{n_c}(\boldsymbol{x}_{ji} - \bar{\boldsymbol{x}}_j)(\boldsymbol{x}_{ji} - \bar{\boldsymbol{x}}_j)^{\mathrm{T}}, \tag{2}$$

where $\boldsymbol{x}_{ji} \in \mathbb{R}^{m\times 1}$ is the vector of the i-th trial for material j, and $\bar{\boldsymbol{x}}_j \in \mathbb{R}^{m\times 1}$ is the mean vector for material j. c is the number of materials, and n_c is the number of samples belonging to each material. $\boldsymbol{S}_w$ represent the variance of samples in each material; thus, the smaller the variance, the easier the classification. The second measure is the between-material scatter matrix $\boldsymbol{S}_b$, which is defined as

$$\boldsymbol{S}_b = \sum_{j=1}^{c}(\bar{\boldsymbol{x}}_j - \bar{\boldsymbol{x}})(\bar{\boldsymbol{x}}_j - \bar{\boldsymbol{x}})^{\mathrm{T}}, \tag{3}$$

where $\bar{\boldsymbol{x}} \in \mathbb{R}^{m\times 1}$ is the mean vector of all samples. $\boldsymbol{S}_b$ represents the distances between the mean vectors of each material and all samples; thus, the larger this value, the easier the classification. LDA determines the feature vectors that maximize the variance of $\boldsymbol{S}_b$ against $\boldsymbol{S}_w$. This calculation involves the eigen value expansion of $\boldsymbol{S}_w^{-1}\boldsymbol{S}_b$.

We extracted the principal components of all samples using PCA before conducting classification with LDA to filter out the insignificant signals as a noise. We applied LDA to the sample set approximated by 19 principal components. They explained approximately 80% of the variance of the original data.

In this study, the feature vectors were computed from either or both the phase differences between the two axial forces ($m = 301$ dimensions) and the power spectra of the shear forces ($m = 300$ dimensions) induced when the 14 participants stroked the 19 types of materials (i.e., $n = 266$ samples). We evaluated the material classification performances using the first 2–30 extracted feature vectors ($d = 2, \cdots, 30$) by applying LDA to the reduced data.

When both phase differences and power spectra were used, their scales were unified before computing their feature vectors. The phase difference $\boldsymbol{\phi}_k \in \mathbb{R}^{301\times 1}(k = 1, 2, \cdots, 266)$ and power spectra $\boldsymbol{p}_k \in \mathbb{R}^{300\times 1}(k = 1, 2, \cdots, 266)$ in the k-th trial were transformed into the z-score in each trial. Then, we applied the PCA and LDA to

$$\boldsymbol{X}_{\phi p} = [(\boldsymbol{\phi}_1\ \boldsymbol{\phi}_2\ \cdots\ \boldsymbol{\phi}_{266})^{\mathrm{T}}\ (\boldsymbol{p}_1\ \boldsymbol{p}_2\ \cdots\ \boldsymbol{p}_{266})^{\mathrm{T}}]. \tag{4}$$

D. Material classification

If the phase differences and power spectra represent the surface properties of materials, then the materials can be classified using this information. Therefore, we investigated whether the materials can be classified in the feature vector spaces extracted by either or both the phase differences and the power spectra by using two popular but distinctive approaches.

The first approach was intended to statistically classify the materials. We applied multivariate analysis of variance (MANOVA) to the pairs of materials in the feature vector space and judged whether arbitrary pairs of two materials could be statistically distinguished. When the results of MANOVA satisfied $p < 0.05$, we judged that the two materials could be distinguished. We calculated the proportion of the distinguished pairs among the whole pairs of the materials. We performed this process for each d $(= 2, \cdots, 13)$. $d = 13$ is the maximum dimension that is adaptable for MANOVA considering the degree of freedom.

The second approach to classify the materials was based on the k-means method, and in this case, we calculated the correct rate of classification [11]. We randomly divided 14 participants into groups A and B with replacement and calculated the centers of the distributions of all 19 materials in each group. Each material in group A was classified as the material in group B that was distributed the closest (k-means method). This judgement was based on the Euclidean distance between the centers of the distributions. This calculation was repeated 100 times, and we computed the mean of the correct rate among all the materials. This calculation was performed for each d $(= 2, \cdots, 30)$.

IV. Results

Fig. 4 (a) exhibits the relationship between the number of feature dimensions d and proportion of the pairs of materials classified by

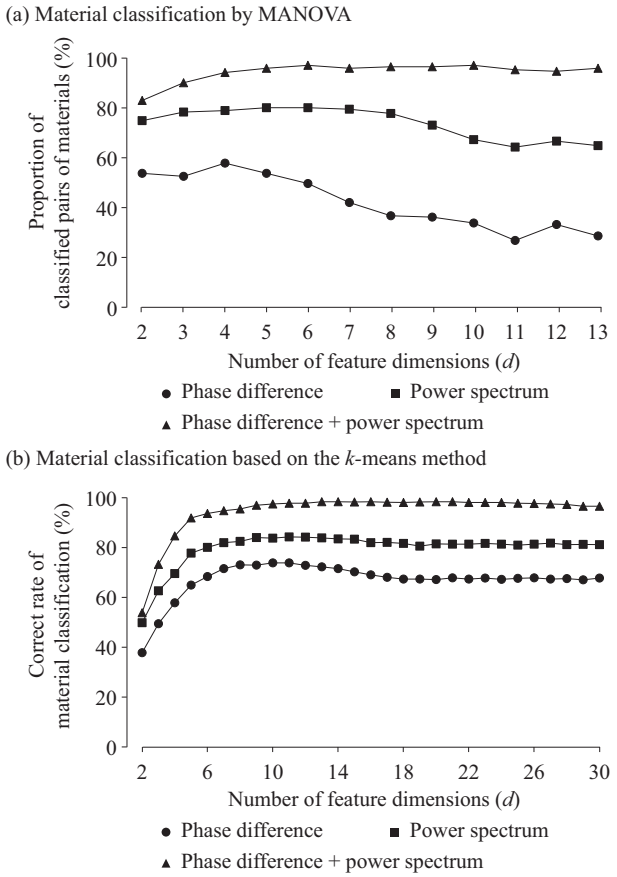

Fig. 4. Classification performance in d-dimensional feature space. (a) Proportion of pairs of materials distinguished by applying MANOVA. (b) Correct rate of classification based on the k-means method.

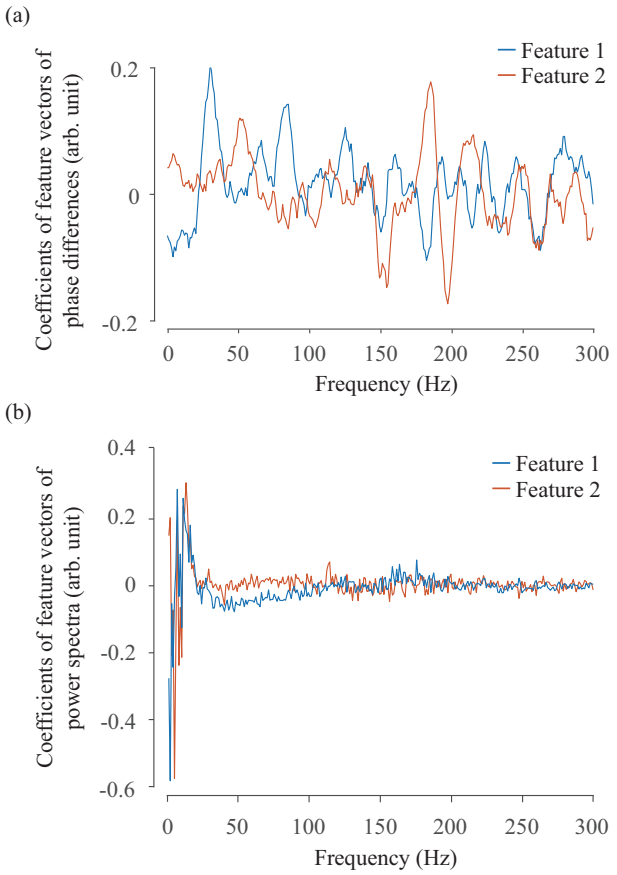

Fig. 5. Coefficients of two feature vectors extracted from the spectra. The feature vectors of (a) phase differences between the two axial forces and (b) power spectra of the shear forces.

MANOVA. At most, 57.9% ($d = 4$) and 80.1% ($d = 5, 6$) of material combinations were distinguished by the phase differences and power spectra, respectively. The corresponding result when both the phase differences and power spectra were used was 97.1% ($d = 10$). The material classification performance when using the power spectra surpassed that of the classification by the phase differences. It is notable that the phase difference represents the differences among the materials though it is inferior to the power spectra in terms of classification performance. The classification performance when both the phase differences and power spectra were used was the highest among the three conditions for all d.

Fig. 4 (b) exhibits the relationship between d and the correct rate of material classification based on the k-means method. The correct rate converged to approximately 70% and 80% using the phase differences and power spectra, respectively, as d becomes larger. The corresponding result was approximately 98% when both the phase differences and power spectra were used. Thus, the features of the materials can be represented better using both the phase differences and the power spectra.

Although similar analyses were performed for the phase differences and power spectra at the frequency resolution $\Delta f = 2$ Hz, the results did not change considerably for both types of criteria. Thus, the frequency resolution may not greatly influence material classification performance.

We introduce the first two feature vectors as the representative examples in the following paragraphs. The contribution ratios of each feature vector of the phase differences were 31.0% and 17.9%, respectively. The corresponding results of the power spectra were 36.8% and 18.7%, respectively. Fig. 5 (a) shows the feature vectors extracted from the phase differences between the two axial forces. They were difficult to interpret, and the coefficients were either positive or negative depending on the frequency range. Fig. 5 (b) shows the feature vectors extracted from the power spectra of the shear forces. They were apparently different up to 100 Hz.

Figs. 6 (a), (b), and (c) show the distribution of the studied materials in the two-dimensional feature vector space computed using phase differences, power spectra, and both, respectively. The sizes of the ellipsoids show the standard errors among all the participants. The smaller the size, the smaller the individual differences. The colors and numbers of the ellipsoids correspond to the types of materials. Although the distribution of the materials differed between the feature vector spaces of the phase differences and power spectra, similar types of materials were found to be distributed together in both spaces (e.g., clothes and papers were distributed in the third and first quadrants, respectively, in the phase difference space, and in the first and second quadrants, respectively, in the power spectrum space). The distributions of the materials in Figs. 6 (b) and (c) were similar. Thus, the effect of the power spectrum was dominant compared to that of the phase difference in the material classification.

Table II shows the breakdown of the number of material pairs classified by MANOVA in the two-dimensional feature space extracted from either the phase differences or the power spectra. The supplementary file shows the final combinations of the classified materials. As shown in Table II, among the 92 pairs of material combinations that were classified by the phase differences, 74 pairs were also classified by the power spectra. This number is equivalent to

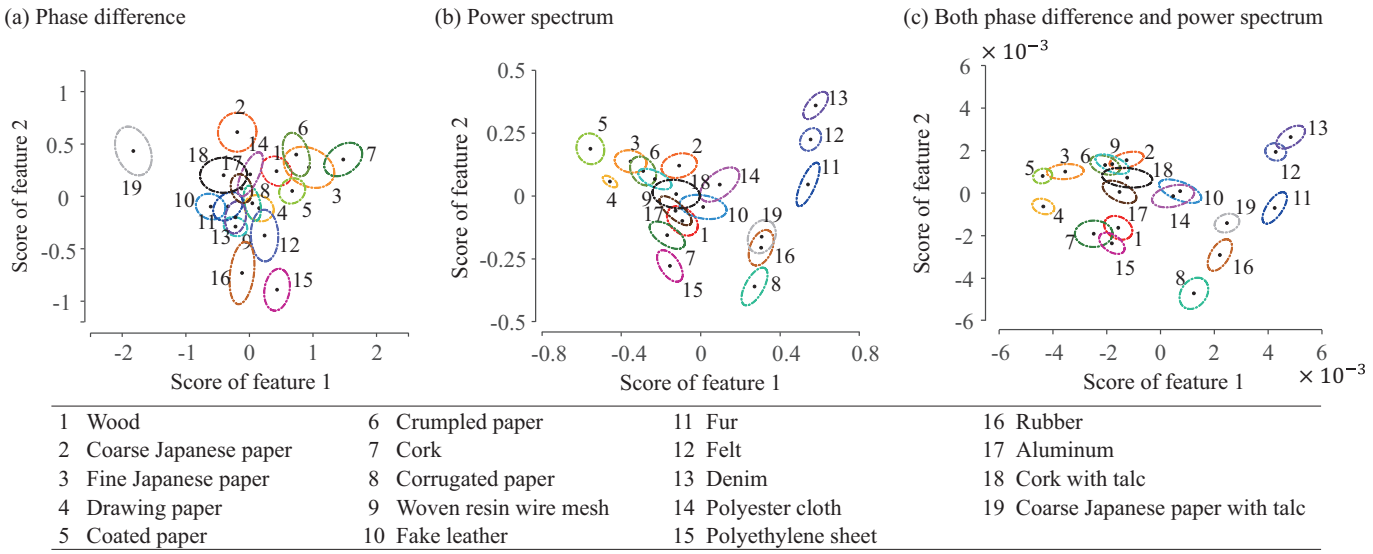

1 Wood	6 Crumpled paper	11 Fur	16 Rubber
2 Coarse Japanese paper	7 Cork	12 Felt	17 Aluminum
3 Fine Japanese paper	8 Corrugated paper	13 Denim	18 Cork with talc
4 Drawing paper	9 Woven resin wire mesh	14 Polyester cloth	19 Coarse Japanese paper with talc
5 Coated paper	10 Fake leather	15 Polyethylene sheet	

Fig. 6. Distribution of materials on the two-dimensional feature vector space computed using (a) phase differences of the two axial forces, (b) power spectra of the shear forces, and (c) both (a) and (b). The sizes of the ellipsoids show the standard errors among the participants. The material numbers correspond to those in the list below.

TABLE II
NUMBER OF MATERIAL PAIRS CLASSIFIED IN TWO-DIMENSIONAL FEATURE SPACE BY MANOVA USING EITHER PHASE DIFFERENCES OR POWER SPECTRA.

		Classified by phase differences		
		Yes	No	Total
Classified by power spectra	Yes	74	54	128
	No	18	25	43
	Total	92	79	

approximately 80% of the material combinations that were classified by the phase differences. However, the remainder of the 18 pairs (∼20%) were classified by the phase differences but not by the power spectra. The phase difference represents differences among materials in a manner unlike the power spectrum, even though its material classification performance was inferior to that of the latter.

V. DISCUSSION

More types of materials were classified using both phase differences and power spectra than using only the latter. The cloth materials were especially well classified when using the power spectra, whereas the other materials were classified well when using both the power spectra and phase differences (Figs. 6 (b) and (c)). This suggests that the features of the materials that cannot be represented by the power spectra can be supplementally represented by the phase differences. Although it is unclear what kinds of properties are represented by the phase difference, the surface property information of materials can be considered to be contained in both the power spectrum and the phase difference, and the latter deserves more focus. Furthermore, when we computed the phase spectra of either the normal or the shear forces during the tactile exploration, they appeared to be random and non-locked, unlike the results seen in Fig. 3 (a). The differences among the materials appear with regard to the phase information of multidimensional signals, such as the phase difference between the normal and shear forces, but not with regard to that of unidimensional signals. It is thus important to investigate not only unidimensional signals but also the relationships between these multidimensional signals.

In this study, the materials were classified by the phase differences and power spectra even though the scanning speeds of the participants' fingers showed some variability (30–90 mm/s) in the analysis. In [11], 55 types of materials were classified using the power spectra of skin vibration induced by scanning the materials at a constant speed under a passive touch condition. Their classification accuracies were 80–93%. In [30], six types of materials were classified using the power spectra of the shear forces while the finger speed was in the narrow ranges under an active touch condition. Their classification accuracies exceeded 90%. The corresponding result of ours was 80%, which may be smaller than those in [11], [30]. The number and types of materials were different among these three studies. Thus, we cannot compare these results directly but in our study the variability in the scanning speed might have had a negative impact on the classification performance.

The classification performances by MANOVA using either the phase differences or the power spectra were maximized at $d = 4-6$ and decreased as d exceeded these values (Fig. 4 (a)). This result may be attributed to signal noise extraction as high-dimensional feature vectors. In general, it is difficult to conduct classification using MANOVA when the data include large amounts of noise. This problem may be similar to overfitting, which may not have occurred when both the phase differences and power spectra were used because the number of variables was larger in this case than when only one of them was used. Thus, the classification performance might have been maintained for a large d. On the other hand, the correct rate of material classification based on the k-means method was high for a large d in all three conditions (Fig. 4 (b)). The noise may not likely influence the k-means method because it uses the distances between the centers of the material distributions.

As shown in Fig. 3 (a), ϕ took both positive and negative values. This result means that the phase of the shear force leads or lags that of the normal force. The former can be explained geometrically. The shear force induced by stroking an uneven surface can be expressed as the derivative of surface displacement [32], [33]. Simultaneously, the normal force can be expressed as the function of surface displacement. This means that the phase of the shear force leads that of the normal force. The delay in the phase of the shear force may be attributed to the behavior of the coupled system in the normal and

tangential directions with viscoelastic resistance.

VI. Conclusion

Most previous studies demonstrated that the power spectra of contact forces or skin deformation induced during tactile exploration represent differences among materials. However, their phase spectra were disregarded because they are not locked and behave randomly. It is reasonable to suppose that the phase differences of two axial forces can be physically determined. Our experiments to this effect showed that the phase differences between them are not random and differ statistically among materials. Among the 19 types of materials, 80% and 58% of the pairs were statistically distinguished by the power spectra and phase differences, respectively. The corresponding results of classification accuracy were 80% and 70%, respectively. Some materials were only classified by the phase difference, and thus, its importance should be reconsidered for understanding tactile material perception and developing tactile texture displays. The correspondence between the phase difference of two axial forces and perception should also be directly investigated in the future.

References

[1] A. M Smith, C. Elaine Chapman, M. Deslandes, J.-S. Langlais, and M.-P. Thibodeau, "Role of friction and tangential force variation in the subjective scaling of tactile roughness," *Experimental Brain Research.*, vol. 144, pp. 211–23, 2002.

[2] M. Wiertlewski, C. Hudin, and V. Hayward, "On the 1/f noise and non-integer harmonic decay of the interaction of a finger sliding on flat and sinusoidal surfaces," in *Proceedings of IEEE World Haptics Conference*, 2011, pp. 25 – 30.

[3] M. Janko, R. Primerano, and Y. Visell, "On frictional forces between the finger and a textured surface during active touch," *IEEE Transactions on Haptics*, vol. 9, no. 2, pp. 221–232, 2015.

[4] X. Zhou, J. Liang Mo, Y. Yuan Li, J. Ye Xu, X. Zhang, S. Cai, and Z. Min Jin, "Correlation between tactile perception and tribological and dynamical properties for human finger under different sliding speeds," *Tribology International*, vol. 123, pp. 286 – 295, 2018.

[5] J. Platkiewicz, A. Mansutti, M. Bordegoni, and V. Hayward, "Recording device for natural haptic textures felt with the bare fingertip," in *Haptics: Neuroscience, Devices, Modeling, and Applications*, M. Auvray and C. Duriez, Eds. Springer Berlin Heidelberg, 2014, pp. 521–528.

[6] Y. Tanaka, W. M. Bergmann Tiest, A. M. L. Kappers, and A. Sano, "Contact force and scanning velocity during active roughness perception," *Plos one*, vol. 9, no. 3, pp. 1–11, 2014.

[7] M. Wiertlewski, J. Lozada, and V. Hayward, "The spatial spectrum of tangential skin displacement can encode tactual texture," *IEEE Transactions on Robotics*, vol. 27, pp. 461 – 472, 2011.

[8] S. Sato, S. Okamoto, Y. Matsuura, and Y. Yamada, "Wearable finger pad deformation sensor for tactile textures in frequency domain by using accelerometer on finger side," *ROBOMECH Journal*, vol. 4, no. 19, 2017.

[9] S. Bensmaïa and M. Hollins, "Pacinian representation of fine surface texture," *Perception & Psychophysics*, vol. 67, pp. 842–54, 2005.

[10] A. I. Weber, H. P. Saal, J. D. Lieber, J.-W. Cheng, L. R. Manfredi, J. F. Dammann, and S. J. Bensmaïa, "Spatial and temporal codes mediate the tactile perception of natural textures," *Proceedings of the National Academy of Sciences*, vol. 110, no. 42, pp. 17 107–17 112, 2013.

[11] L. R. Manfredi, H. P. Saal, K. J. Brown, M. C. Zielinski, J. F. Dammann, V. S. Polashock, and S. J. Bensmaïa, "Natural scenes in tactile texture," *Journal of Neurophysiology*, vol. 111, no. 9, pp. 1792–1802, 2014.

[12] R. Fagiani, F. Massi, E. Chatelet, Y. Berthier, and A. Akay, "Tactile perception by friction induced vibrations," *Tribology International*, vol. 44, no. 10, pp. 1100 – 1110, 2011.

[13] I. Cesini, J. D. Ndengue, E. Chatelet, J. Faucheu, and F. Massi, "Correlation between friction-induced vibrations and tactile perception during exploration tasks of isotropic and periodic textures," *Tribology International*, vol. 120, pp. 330 – 339, 2018.

[14] L. Skedung, K. Danerlöv, U. Olofsson, C. Michael Johannesson, M. Aikala, J. Kettle, M. Arvidsson, B. Berglund, and M. Rutland, "Tactile perception: Finger friction, surface roughness and perceived coarseness," *Tribology International*, vol. 44, pp. 505–512, 2011.

[15] Y. Matsuura, S. Okamoto, H. Nagano, and Y. Yamada, "Multidimensional matching of tactile sensations of materials and vibrotactile spectra," *Information and Media Technologies*, vol. 9, no. 4, pp. 505–516, 2014.

[16] S. Okamoto and Y. Yamada, "An objective index that substitutes for subjective quality of vibrotactile material-like textures," in *Proceedings of IEEE/RSJ International Conference on Intelligent Robots and Systems*, 2011, pp. 3060–3067.

[17] T. Yoshioka and J. Zhou, "Factors involved in tactile texture perception through probes," *Advanced Robotics*, vol. 23, no. 6, pp. 747–766, 2009.

[18] M. Strese, C. Schuwerk, and E. Steinbach, "Surface classification using acceleration signals recorded during human freehand movement," in *Proceedings of IEEE World Haptics Conference*, 2015, pp. 214–219.

[19] A. Burka and K. J. Kuchenbecker, "Handling scan-time parameters in haptic surface classification," in *Proceedings of IEEE World Haptics Conference*, 2017, pp. 424–429.

[20] S. Ding, Y. Pan, M. Tong, and X. Zhao, "Tactile perception of roughness and hardness to discriminate materials by friction-induced vibration," *Sensors*, vol. 17, no. 12, 2017.

[21] W. Tang, N. Chen, J. Zhang, S. Chen, S. Ge, H. Zhu, S. Zhang, and H. Yang, "Characterization of tactile perception and optimal exploration movement," *Tribology Letters*, vol. 58, 2015.

[22] J. Edwards, J. Lawry, J. Rossiter, and C. Melhuish, "Extracting textural features from tactile sensors," *Bioinspiration & Biomimetics*, vol. 3, no. 3, 2008.

[23] E. Kerr, T. McGinnity, and S. Coleman, "Material recognition using tactile sensing," *Expert Systems with Applications*, vol. 94, pp. 94 – 111, 2018.

[24] S. Bensmaïa and M. Hollins, "Complex tactile waveform discrimination," *Journal of the Acoustical Society of America*, vol. 108, pp. 1236–1245, 2000.

[25] S. A. Cholewiak, K. Kim, H. Z. Tan, and B. D. Adelstein, "A frequency-domain analysis of haptic gratings," *IEEE Transactions on Haptics*, vol. 3, no. 1, pp. 3–14, 2010.

[26] K. Horch, "Coding of vibrotactile stimulus frequency by pacinian corpuscle afferents," *Journal of the Acoustical Society of America*, vol. 89, pp. 2827–2836, 1991.

[27] S. Kuroki and S. Nishida, "Human tactile detection of within- and inter-finger spatiotemporal phase shifts of low-frequency vibrations," *Scientific Reports*, vol. 8, no. 4288, 2018.

[28] H. Hasegawa, S. Okamoto, H. Elfekey, and Y. Yamada, "Stochastic relationships between the normal and shear interaction forces during tactile exploration of textures," in *Proceedings of IEEE International Conference on Systems, Man, and Cybernetics*, 2018, pp. 3033–3038.

[29] S. Okamoto, M. Wiertlewski, and V. Hayward, "Anticipatory vibrotactile cueing facilitates grip force adjustment during perturbative loading," *IEEE Transactions on Haptics*, vol. 9, no. 2, pp. 233–242, 2016.

[30] R. V. Grigorii, M. A. Peshkin, and J. E. Colgate, "High-bandwidth tribometry as a means of recording natural textures," in *Proceedings of IEEE World Haptics Conference*, 2017, pp. 629–634.

[31] D. L. Swets and J. J. Weng, "Using discriminant eigenfeatures for image retrieval," *IEEE Transactions on Pattern Analysis and Machine Intelligence*, vol. 18, no. 8, pp. 831–836, 1996.

[32] G. Robles-De-La-Torre and V. Hayward, "Force can overcome object geometry in the perception of shape through active touch," *Nature*, vol. 412, pp. 445–448, 2001.

[33] Y. Fujii, S. Okamoto, and Y. Yamada, "Friction model of fingertip sliding over wavy surface for friction-variable tactile feedback panel," *Advanced Robotics*, vol. 30, no. 20, pp. 1341–1353, 2016.